In Press since Feb. 2020

Characteristics of downslope windstorms in the view of the typical atmospheric boundary layer

Hrvoje Kozmar[1] and Branko Grisogono[2]

[1]Faculty of Mechanical Engineering and Naval Architecture, University of Zagreb,

Ivana Lučića 5, 10000 Zagreb, Croatia

[2]Department of Geophysics, Faculty of Science, University of Zagreb,

Horvatovac 95, 10000 Zagreb, Croatia

Abstract: There is a clear need to learn more about the exact characteristics of downslope windstorms in order to accurately address relevant topics in environmental aerodynamics and wind engineering. In particular, the characteristics of the atmospheric boundary layer are well known and provided in international standards and textbooks; however, further work is required to elucidate characteristics of downslope windstorms and make them available in a form suitable for engineering applications. While downslope windstorms have been successfully addressed in the meteorology, climatology and geophysics communities, the focus of those groups is quite different than in wind engineering, i.e. the existing data on characteristics of downslope windstorms are of marginal relevance for engineering applications. It is therefore the scope of this chapter to provide a critical review of the state-of-the-art on characteristics of those local and unique winds in comparison with the typical atmospheric boundary layer. It is expected that this work will encourage a more detailed codification of those winds. Another important goal is to enhance an interdisciplinary collaboration among the meteorology, geophysics and engineering communities because it is shown in this chapter that the current wind engineering standards do not entirely keep up with the atmospheric physics of downslope windstorms.

1. INTRODUCTION

Civil engineering infrastructure has been commonly designed according to relevant standards and codes - this is obligatory for the contractors and the owners. An important portion of those standards and codes focuses on wind-induced damage and structural collapse, whereas the wind characteristics are, for the most part, represented as the atmospheric boundary layer (ABL). At the same time, only in the North America it has been observed that 65% of the wind-induced damage is due to non-synoptic, local windstorm events that may be very different than the ABL.

At this moment, there are no clear guidelines or code implementations on the characteristics of local, mountainous windstorms. It is therefore of great interest to learn more about those winds and provide their characteristics in a form usable for engineers. The windstorms in mountainous regions have been previously thoroughly assessed in the meteorology and geophysics communities; however, their focus is quite different than

in the wind engineering, and the available data on characteristics of mountainous windstorms are of marginal relevance for engineering applications.

Some people say, consider the Earth greatly downscaled to a tennis ball, it will be smoother than a billiard ball. But there is a crux: the relevant atmosphere here is shallow, its density scale is only about 8.5 km deep compared to e.g., the Earth radius; thus, it is extremely sensitive to vertical motions, at least for two major reasons. One is high amounts of water vapor, so that any vertical motion might lead to air saturation, eventual condensation and deep convection including organized, non-synoptically driven air-flows such as multi-cells, super-cells, squall-lines, mesoscale meteorological systems and more (these may generate e.g., tornadoes, flash-flooding, etc.). Another reason - largely the subject of this chapter, is that generally strong static stratification of the atmosphere, which also keeps the air close to the Earth, generates buoyancy waves and resists vertical motions (e.g., Smith 1979, 1985). Hence, the air must often undertake large horizontal excursions and, when inevitable, it yields strong to severe downslope winds, which may easily exceed hurricane speeds (> 33 m/s) and generate severe turbulence near the surface and aloft. Meanwhile, the world population is largely affected by mountainous conditions because mountains cover 25 % of the Earth's surface, they are home to 26 % of the world total population and generate 32 % of the surface runoff; moreover, plateaus and hills cover another 21 % of the Earth's surface, contain additional 20 % of the population and yield 19 % of the runoff (e.g., Chow et al. 2013).

Different yet significant, regionally decisive air-flows are generated by mountains; these are usually segregated into thermally driven (e.g., katabatic and anabatic winds with wind speed commonly smaller than 10 m/s, except for Antarctica) and dynamically (mechanically) driven circulations (e.g., Bora, Chinook, Foehn, Helm, Mistral, Santa Ana, Zonda, etc.). For recent review of the former type, see Zardi and Whiteman (2013); for the latter type, see Jackson et al. (2013) and a special issue of WAS (2017). These winds, especially severe downslope windstorms, together with the related gap winds and cold-air pools, determine the ABLs local properties, loads on engineering structures, dispersion of pollutants, road safety and overall traffic, crop damage and more (e.g., Baklanov et al. 2011). To reword, strong downslope windstorms related to large-amplitude mountain waves (e.g., severe Foehn) can easily cause significant damage which is typically not considered by engineering design, standards and codes.

Simultaneously, these mountain-wave breakings in the atmosphere are most often related to wild hydraulic-like jumps (e.g., Klemp and Durran 1987, Smith 1987, Dörnbrack 1998, Enger and Grisogono 1998) and/or rotors, even with dangerous sub-rotors with excessive turbulence, in the lee of mountains (Doyle and Durran 2004, 2007, Doyle et al. 2009), or roll vortices with horizontal wavelength of ~ 1 km, comparable to the corresponding ABL depth, which generate a great variability of wind speeds over short distances, comparable to street sizes or less. Rotors (intense low-level vortices with horizontal rotation axis that are observed parallel and downstream of a mountain related to large-amplitude mountain wave) immediately correspond to the adverse pressure gradient in the mountain lee, due to large-amplitude waves, yielding to the ABL separation and more (e.g., Grubišić and Billings 2008, Sachsperger et al. 2015, Strauss et al. 2016). In fact, one of the most important recent mega-projects related to mountainous severe weather, is T-REX, summarized by Grubišić et al. (2008). In T-REX, the most advanced observational and modeling tools assessing airflows from the Earth surface to the lower stratosphere over the Sierra Nevada, USA, were used to unveil wild rotors in the air (see e.g., https://www.eol.ucar.edu/node/666/publications). It is appealing that such rotors, induced by strong-to-severe

downslope winds, were already studied more than 130 years ago by the geophysical community (Mohorovičić 1889) and as a follow-up (Grubišić and Orlić 2007); however, so far those winds have not been accordingly considered by the engineering standards and codes.

For a review of stratified airflow over orography see Smith (2002). A fresh and timely set of papers related to mountainous weather is compiled by Teixeira et al. (2016). It is indicated there that field campaigns like MAP, T-REX, Materhorn, COLDPEX and i-Box, containing a wealth of mountain meteorology measurements are only starting to be in-depth explored. That should lead to important advances in understanding weather in mountainous regions, as well as mixing and pollutant dispersion over complex terrain. The latter is sometimes still mistreated by the geophysical community by using a first-order K-theory for parameterizing turbulent fluxes, which is not appropriate for that purpose (e.g., Pope 2000, Wyngaard 2010).

The scope of the present chapter is to address characteristics of some major mountainous winds in comparison with the standard ABL, i.e. Santa Ana (West Coast of North America), Foehn (European Alps), downslope winds of Liguria (Europe), Bora (Adriatic Region in Europe), downslope winds of Japan (Asia), Zonda (Andes in Latin America). The presented information is expected to enhance creating a platform for implementing the characteristics of local mountainous winds in the international standards and codes. Structurally, we opted for a scientific review study instead of a pure or applied corresponding timely paper, for which there is ample of results in terms of field campaigns, laboratory experiments and advanced computational simulations. The option chosen is because the community yearns urgently for a better leveling off and a better mutual correspondence between the engineering and geophysical, say, meteorological and climatological communities due to rapid recent climate changes, for an optimized collaboration, for better mutual shares in education, just to mention a few.

2. THE ESSENCE OF MOUNTAINOUS WINDSTORMS

Although interactions between thermally forced and mechanically (dynamically) driven airflows are possible, and in fact such interactions are ubiquitous during the course of the day (e.g., Poulos et al. 2000, 2007), it appears that the latter flow type is generally stronger (e.g., Smith 1979, Chow et al. 2013). Hence, we focus on that.

To put it most boldly and simply, those most severe downslope winds appear wherever a resonance between the incoming stratified flow (wind speed U and buoyancy frequency N) and the underlying orography (height H), e.g., an elongated mountain, occurs (leave aside various often secondary yet important details, such as the width and length of the mountain, eventually multilayered atmosphere, etc.). Vertical Froude number, $Fr = U/(NH)$, or its inverse, which is dimensionless mountain height, $\hat{H} = HN/U$, describes the resonance. Typically, for $0.15 \leq Fr \leq 1.2$, large mountain waves break due to the resonance (e.g., Smith 1985, 1987, Klemp and Durran 1987, Ólafsson and Bougeault 1996, Hunt et al. 1997) and produce severe winds below wave-breaking region, Fig. 1.

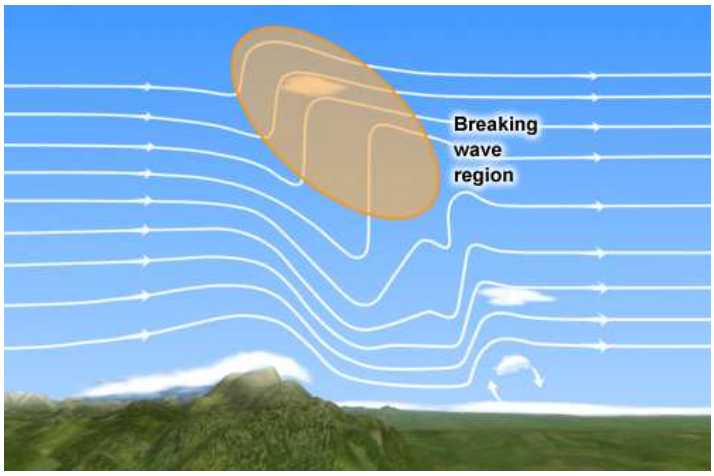

Figure 1. Sketch of a large mountain-wave that breaks. Downslope windstorm occurs in the lee of the mountain where the streamlines are the closest, there and below is a shooting flow. The corresponding supercritical flow usually ends with a hydraulic-like jump, or an undular bore, both sometimes followed by a rotor (also drawn). The sketch originally provided for Boulder-Denver, CO, USA, windstorm also applies to other similar winds such as Bora, Foehn, Santa Ana, Sierra Nevada windstorms, windstorms of Japan, etc. wherever noticeable flow blocking occurs. Source: COMET UCAR/NCAR, USA educational website.

At the lower range of those critical Froude numbers, wave-breaking occurs only at the flanks of mountains and is more localized. Somewhat above that critical range of Fr, waves only steepen but do not overturn and break. For $Fr \geq 2$, the mountain waves become increasingly linear and smooth, without patches of turbulence. Almost needless to say, the linear wave theory cannot explain mountain-wave breaking (e.g., Smith 1979); the theory is practically invalid for $Fr \leq 1$, theoretically even before, the quantitative errors may go beyond a factor of two and more; yet, some qualitative points based on the linear wave theory are still valid (e.g., Hunt et al. 1997, Smith 2002). It is conceivable, understandable and theoretically proven that for mountain shapes prone to yield severe downslope windstorms, their height on the windward site should gradually increase, so that a strong standing wave can build up (for a ridge H = 1 km, 20 km wide, typical U = 10 m/s and N = 0.01/s, it takes about three hours to make a strong mountain wave, based on a rough hydrostatic estimate of the vertical component of the wave group velocity); on the contrary, the lee side ought to be rather steep (Smith 1977, 1979, Lilly and Klemp 1979). All that is closely related to significant airflow blockings by orographical obstacles.

Mountain pressure drag (MPD) is one of the best measures of mountain effects, including nonlinearities and gross turbulence, on incoming stratified airflows (Smith 1978, Teixeira et al. 2008, Teixeira, 2014). It is an integral of the horizontal pressure difference over a mountain in the main wind direction perpendicular to the mountain. The point is that for severe downslope windstorm values of the MPD, the wave drag is a large contributor to, go by a factor of three and more beyond their linearly corresponding values (Durran 1986, 1990). Unfortunately, the MPD is not readily available from regular numerical weather prediction (NWP) models; however, it can and it should be included as a simple, obtainable and reliable preliminary diagnostics of mountainous weather effects for various engineering applications. Furthermore, the MPD behavior in future climates could be estimated from regional climate models that use horizontal resolution below 10 km. One of the

recommendations of this study is to use the MPD diagnostics and to apply it to certain areas of interest, i.e., to the areas prone to severe windstorms to reliably estimate wind loads on engineering infrastructure.

Going back to the processes tackled, Fig. 2 shows one typical setup with $Fr \sim 0.5$ for severe turbulence in the lee of a mountain. The largest near-surface wind speeds occur in the immediate lee (already discussed) while gusty, unsteady turbulence appears several kilometers further downwind and gradually dies out (not shown) a few tens of kilometers downwind of the obstacle (e.g., Klemp and Lilly 1978, Lilly 1978).

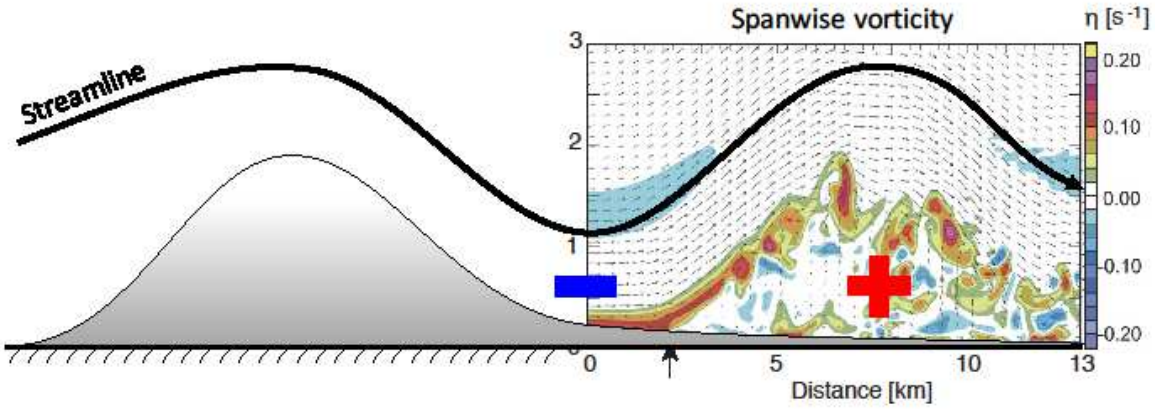

Figure 2. Severe downslope windstorm near the ground (~~blue~~ minus~~,~~ sign corresponding to $U \sim 25$ m/s) ending with a rotor and subrotors around (~~red~~ plus sign). The airflow is from left to right and a large-amplitude mountain wave is generated due to a resonance between the incoming airflow and mountain. Intensive horizontal vorticity snapshot is marked as η ~~in the colorbar~~ having both positive and negative huge values ~ 0.2/s; these are a thousand times larger than a typical vertical (i.e., dominant) value for an atmospheric weather system. Wilderness and severity of this unsteady vorticity is largely due to 3D subrotors and their turbulence; there, vertical accelerations may go up to $\pm 5g$, g is acceleration due to gravity Adapted from Doyle and Durran (2007) and with courtesy of Johannes Sachsperger (2016, personal communication).

In the immediate lee of a mountain where a severe windstorm occurs, there is another plausible yet frequent process that generates additional turbulence – quasiperiodic oscillations in the mean wind speed, i.e., pulsations. These often come from Kelvin-Helmholtz instabilities, i.e., secondary atmospheric waves' instabilities, although other mechanisms are possible as well (Scinocca and Peltier 1993, 1994). The streamline on the right hand side in the lee of the mountain develops upwards similar to a sine function due to the observed complex physical phenomena that include rotors and subrotors. The streamline on the right hand side in the lee of the mountain develops upwards similar to a sine function due to the observed complex physical phenomena that include rotors and subrotors. As an example, Figure 3 shows such pulsations in the Bora wind at the Adriatic Coast. The most exquisite thing about Bora is not its mean wind speed but its frequent gustiness that occurs at several distinct frequency ranges (e.g., Belušić et al. 2007) while reaching hurricane speeds. One way to conceive and comprehend such a shooting flow (e.g., Klemp and Durran 1987) is a variable and a 3D localized low-level jet prone to its own instabilities. It is important to note that Šoljan et al. (2018) show that Bora turbulence properties are independent on the synoptic setup.

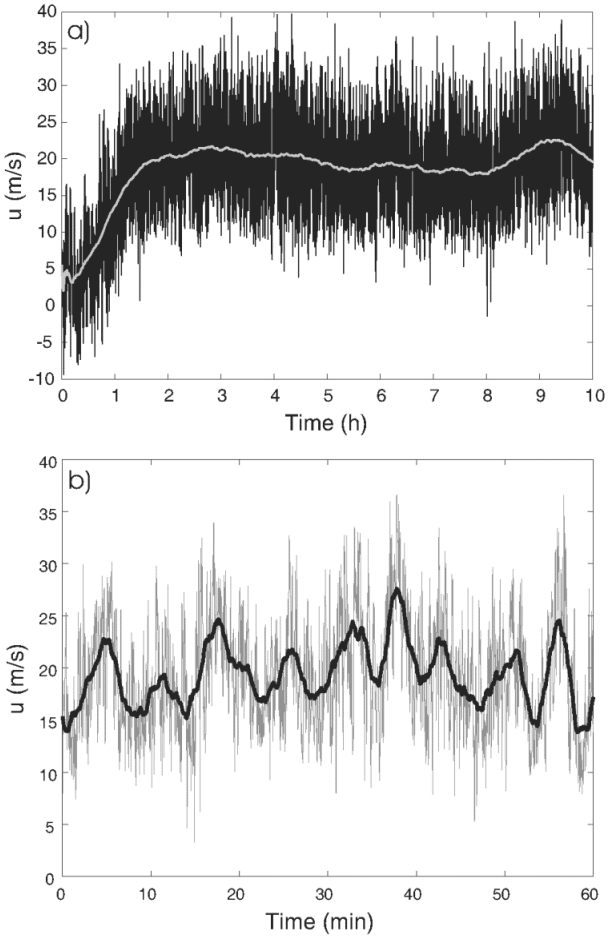

Figure 3. Pulsations of the Bora wind speed, the NE Adriatic Coast, Croatia. The along-Bora wind component in the town of Senj is shown: a) 1-s time series of a part of a Bora episode (black) with 1-h mean superimposed (grey), b) 1-h expanded view of the 6th hour of the episode of the 1-s series (grey) with 2-min mean superimposed (black) showing pulsations. Adapted from Grisogono and Belušić (2009).

Other strong winds can be generated by partial flow separation in the lee of mountains (buoyancy forces negligible), generation of trapped lee waves, upstream blocking of near-surface cold air, and interaction between mountain ridge/range for a stable ABL (Smith 1978, 1979, Chow et al. 2013); the latter two include gap winds and barrier jets. The main feature of gap winds is the asymmetry between the region upstream of the gap entrance and downstream of the gap. The upstream layer flowing through the gap is thick and slow (in hydraulic terminology: subcritical). Approaching the gap, it gets thinner, accelerates and becomes supercritical downstream of the gap. In that sense, especially with maximum $U \sim 25$ m/s, it appears almost as an atmospheric wave breaking phenomenon yielding the severe wind in the lee; however, gap winds do not require a complex vertical airflow structure including stratification effects. We mention barrier jets too, one of at least of four different kinds of tropospheric low-level jets (coastal, nocturnal, etc.), see e.g., Rogers et al. (1998) and Jackson et al. (2013).

In general, low-level jets are important because they transport air properties over long distances, sometimes over thousands of kilometers; moreover, due to their intrinsic instabilities, they may affect ABL properties significantly, through e.g., top-down turbulence (e.g., Wyngaard 2010). Barrier jet is an elevated wind maximum on the windward side of a mountain obstacle that blows parallel to the barrier around the ABL top. Barrier jets appear where stably stratified flow approaches an extra-tropical mountain obstacle and the airflow is blocked by the barrier for hours or longer. Those types of winds are typically but not necessarily more localized winds, at least in terms of two coordinates, compared to severe downslope windstorms (e.g., Jackson et al. 2013). Where the mountain range is sufficiently long and perpendicular to the incoming airflow, say, at least 150 km and more, then the rotation of Earth becomes important, namely the Coriolis force (Smith 1979, Hunt et al. 2001).

On the northern hemisphere, when the mean westerly airflow approaches such a long barrier and it inevitably senses a lower pressure on its left hand side, i.e., toward north (due to a geostrophic balance between the pressure gradient force and Coriolis force), it naturally turns there. This causes a stronger airflow at the northern flanks of the barrier, including anticyclonic rotation in the related lee and a relatively stronger low-level jet, all compared to the flow at and after the southern flank of the barrier (cyclonic rotation, a weaker jet and perhaps more humidity). That pertains to e.g., the Rockies in the USA, to some extent to the Scandinavian mountains and the Alps, etc.; however, it is difficult to observe that effect due to numerous other influences, such as detailed orography and incoming airflow structures. The opposite sense of the airflow turning while approaching a significant mountain occurs at the southern hemisphere, e.g., Smith (1979).

It is inconceivable to review all the famous types of severe downslope windstorms and strong gap winds in this chapter. For instance, severe Chinook and Foehn appear with partial or almost complete blocking of the lower troposphere airflow due to 3 km high mountains or even higher; thus, the air from the higher troposphere, or sometimes even from the tropopause or lower stratosphere, must subside to compensate for the blocking (e.g., Lilly 1978, Lilly and Klemp 1979, Smith 1979, Hunt et al. 1997, Richner and Hächler 2013, Mayr et al. 2018). Of course, some of the air flows around the terrain slopes and over its flanks. These winds are usually warm since the air from high aloft has a larger potential temperature than the air in the ABL. A potential release of precipitation may add to that warming. A list of explanations and definitions of Foehn-related terms is given in Richner and Hächler (2013). On the other hand, if the mountains are lower, say $H \sim 1$ km, only a partial airflow blocking may occur.

A typical example for that phenomenon are severe Bora-types of flow. Dynamically speaking, there is no substantial difference in the mechanisms, i.e., all three kinds of downslope windstorms are very similar, although their details vary. Bora-type winds are usually cold. Firstly, because the compensating air from aloft is relatively closer to the ABL, when compared to Chinook and Foehn, so that there is no substantial downslope warming in Bora. Furthermore, Bora (from the old Greek language for northerly flows) usually comes from northerly directions, which are generally cooler ones on the northern hemisphere. To add a point, the Adriatic Bora, that blows more frequently in winter, is usually induced by a high pressure system over the central Europe or/and Siberia, which brings cooler air to the Mediterranean including the Adriatic Sea. There are two other major synoptic setups for Bora, but they also end up with cold winds over the relatively warmer coastal sea in winters, e.g. Jurčec (1981). It is unfortunate that some websites including Wikipedia classify Bora wrongly as a falling, e.g., katabatic wind, instead of a downslope windstorm.

It is interesting that the term 'Bora' is also applied to similar winds in other parts of the world. That includes, but it is not limited to, Novaya Zemlya in the Arctic, Novorossiysk at the northern coast of the Black Sea, the Gulf of Tehuantepec on the Pacific coast of Mexico, Salt fiord and Bals fiord in northern Norway, etc. (e.g. Yoshino 1976). Another curious point about Bora is that it was classified as a downslope windstorm only 31 years ago (Smith 1987, Klemp and Durran 1987). Then the whole concept for this wind changed (from a falling, i.e., mostly thermally-driven flow) into dynamically-forced airflow. The mountain-wave overturning that occurs beneath the temperature inversion appears as the most important factor in producing the strong to severe response. This overturning generates a shooting flow over the lee slope and resembles the hydraulic-like flow, undular bore and more (e.g., Chow et al. 2013, Sachsberger et al. 2015). The next section outlines the most important currently known points on the discrepancies in characteristics of mountain windstorms and the ABL that still remain to be entirely accounted for in the major international engineering standards and codes.

3. DOWNSLOPE WINDSTORMS VS. TYPICAL ATMOSPHERIC BOUNDARY LAYER

Thermal stratification

Thermal stratification in the ABL is a consequence of the balance between the thermally and mechanically induced mixing of airflows in the lower atmosphere. It may substantially influence wind characteristics at small wind velocities, i.e. smaller than 5 m/s, and therefore change patterns in air pollution dispersion and dilution, urban micrometeorology, etc. The ABL thermal stratification can be (very) stable, neutral, or unstable depending on the heat gradient between the ground, water or ice surface and the airflows above it, Fig. 4, see e.g., Serafin et al. (2018).

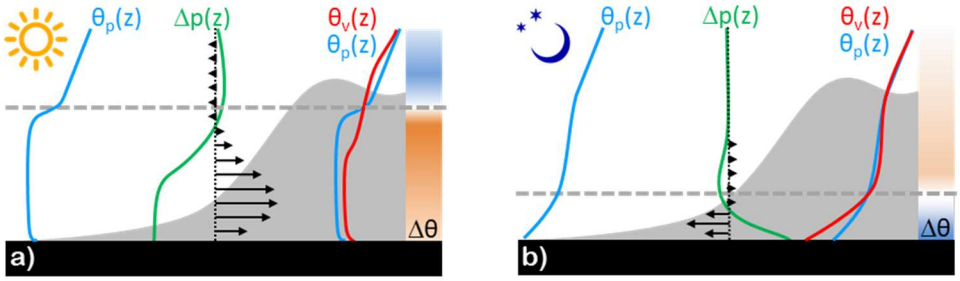

Figure 4. Stable, neutral, and unstable types of ABL thermal stratification (after Serafin et al. 2018); thermally driven winds in a valley with horizontal ground surface. (**a**) During the day, the atmosphere in the valley (~~red profile,~~ ϑ_v profile) is warmer than that over the plain (~~blue profiles,~~ ϑ_p profile). The largest imbalances ($\Delta\vartheta = \vartheta_v - \vartheta_p$) are often found near mountain top level. Horizontal pressure differences ($\Delta p = p_v - p_p$) result quasi-hydrostatically from the vertically integrated temperature imbalances, and are typically largest at the valley ground surface. The wind responds to the pressure gradient and is decelerated by friction near the ground. Deeper convective mixing in the valley causes an elevated cool anomaly, which may drive an upper-level return flow. (**b**) The opposite situation occurs at night.

Rotach and Zardi (2007) describe numerous meteorological and even hydrological issues about the ABL over complex terrain, especially that over the European Alps during the MAP project. Their work is put in a broader perspective by Serafin et al. (2018). One of the key issues there is a frequent inadequacy of the Monin-Obukhov similarity theory (e.g., Grisogono and Oerlemans 2001), which has significant consequences not only for data processing, but also for the NWP and climate models.

Numerous further issues about weather forecasting and regional climate modeling over complex terrain, which is a definitely unsettled problem, were tackled by e.g., Zhong and Whiteman (2008) and Chow et al. (2013). Various issues arise ranging from numerical stability aspects, choice of non-orthogonal coordinate frame, to parameterizations of subgrid scale processes (radiation, clouds, fog, precipitation, (sub)surface processes and turbulence). Figures 5 and 6 add on the ABL complexity by sketching mountainous low-level airflow conditions; needless to say, these situations are uneasy to predict by operational NWP models (e.g., Sun et al. 2015). While Fig. 5 displays frequent multi-layered structure of the ABL over complex terrain including multiple temperature inversions, Fig. 6 sketches the corresponding stably stratified nocturnal ABL. The latter includes, yet it is not limited to, katabatic (thermally-driven downslope) wind, low-level jet, fine-scale turbulence and air-pollution issue.

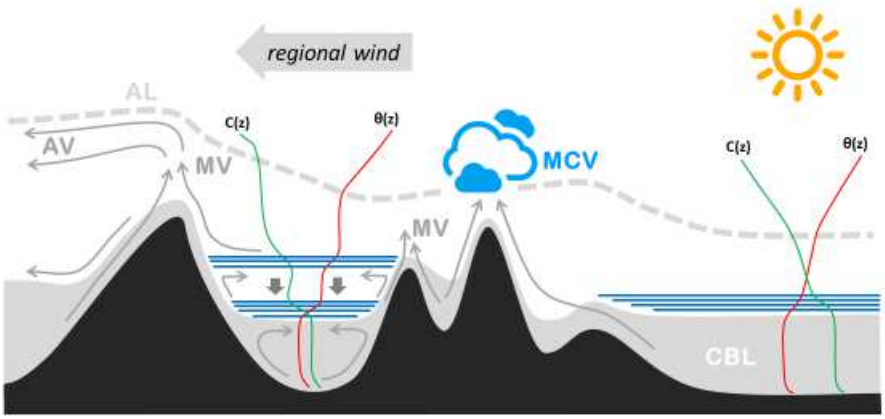

Figure 5. Similar to Fig. 4 but for the ABL over mountainous terrain yielding to numerous flow complexities. Adopted from Serafin et al. (2018). Exchange processes in the daytime boundary layer over mountainous terrain. Grey shading indicates the ground-based mixed layer (CBL). MV, AV, and MCV denote, respectively, mountain venting, advective venting, and mountain-cloud venting. Arrows indicate airflow, while $C(z)$ and $\vartheta(z)$ indicate vertical profiles of pollutant concentration and potential temperature, respectively. Horizontal ~~blue~~ lines represent layers with enhanced static stability, which favor the separation of up-slope flows from the ground. Down-pointing arrows represent valley-core subsidence. The dashed line indicates the top of the regional aerosol layer (AL).

All that may interact with a downslope windstorm (e.g., Poulos et al. 2000, Rotach and Zardi 2007) or even be flushed away (e.g., Jackson et al. 2013).

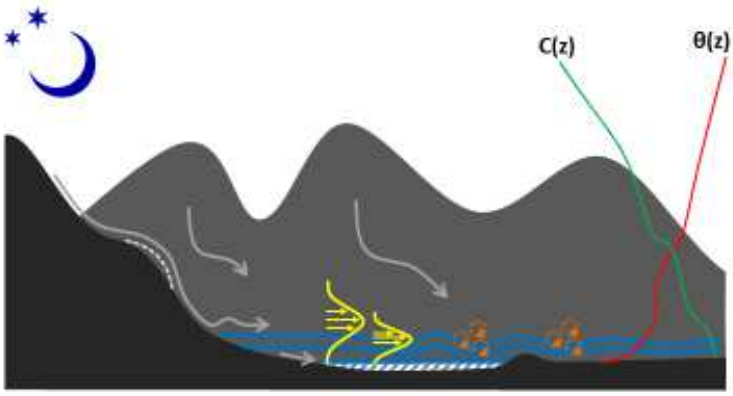

Figure 6. Similar to Figs. 4 and 5 but for the nighttime (stable) ABL over mountainous terrain. A review of interactions between the stable ABL and short buoyancy waves, as indicated here, can be found in Sun et al. (2015). Adopted from Serafin et al. (2018).

On the other hand, there are strong indications that the downslope windstorms are thermally neutrally stratified that is due to an intense mechanical mixing of the airflows as they develop over complex mountainous terrains, whereas the thermal effects are negligible, e.g. Lepri et al. (2014, 2017), Fig 7. In this figure, the thermal stratification is described using the dimensionless parameter ζ, (also called a stability parameter, e.g., Stull, 1988). Positive ζ implies a statically stable stratification, negative ζ implies a statically unstable stratification and ζ equal to zero implies statically neutral stratification. For Bora-like flows (and very likely for other downslope windstorms as well), ζ is nearly zero, statistically speaking, thus indicating the near-neutral thermal stratification of the atmosphere in the 30-min temporary mean surface layer close to ground surface.

Nevertheless, for some other downslope winds, e.g. Santa Ana, various profiles of the potential temperature were observed, e.g. Fig. 8 from Fovell and Cao (2017), where the surface layer static stratification may significantly depart from near-neutrality for a while.

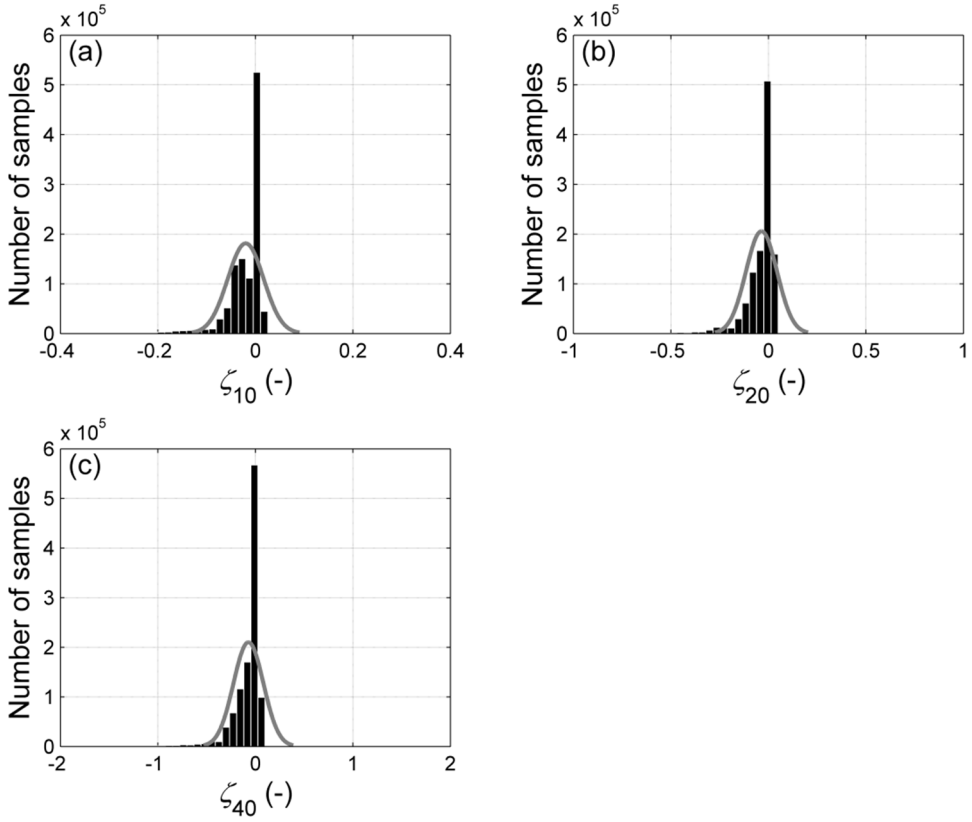

Figure 7. Typical example of statistically neutral static stratification of the atmospheric surface layer in a downslope windstorm; Bora neutral stratification of the atmosphere (Lepri et al. 2014).

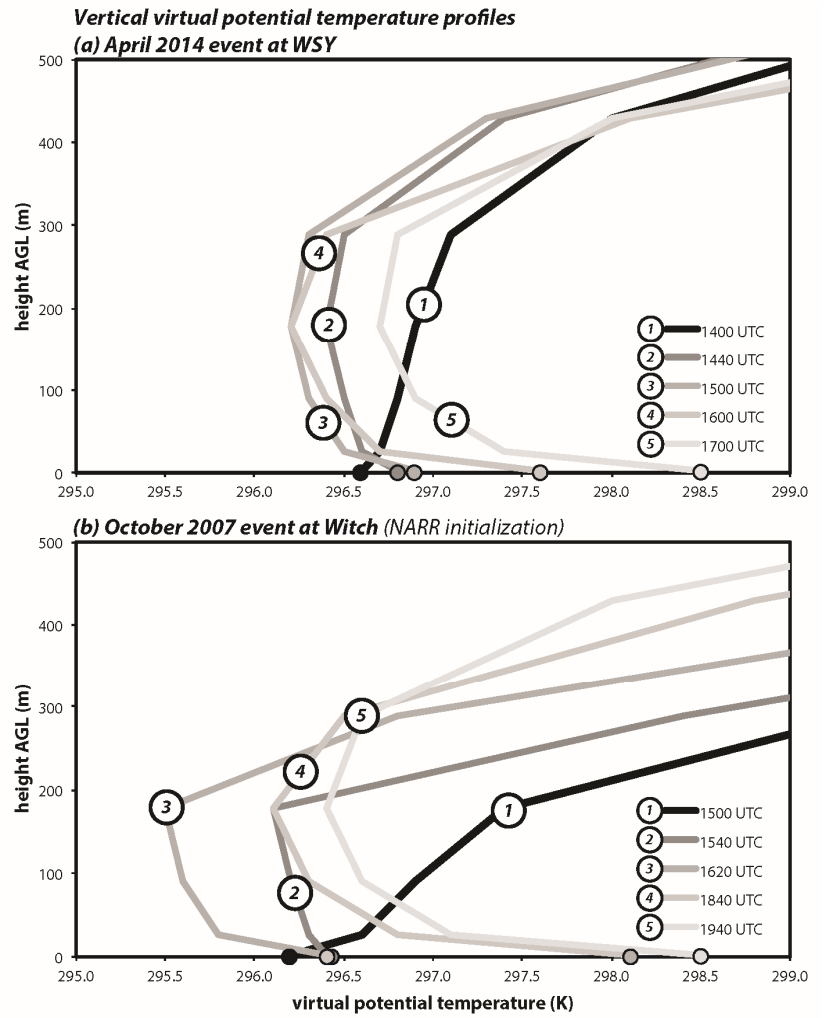

Figure 8. Thermal stratification of a Santa Ana event (Fovell and Cao 2017). Also note that this type of winds promotes wildfires, similar to that due to Bora, Chinook and more.

Wind velocity time history

In wind engineering applications that are commonly performed using experimental, theoretical, and analytical approaches the wind velocity in the ABL is usually taken as quasi steady (e.g. Fig. 9 from Dyrbye and Hansen 1997), as long wave meandering plays little role for wind effects on structures. In the urban environments close to the ground, where the atmospheric turbulence is typically but not necessarily at its maximum, the standard deviation of the ABL velocity fluctuations to the local mean wind velocity (commonly known as the turbulence intensity) is around 40 %, while for downslope windstorms the wind velocity during the wind gust may be five times larger than the mean wind velocity, e.g., Durran (1986).

The fluctuation periods of the flow velocities in the ABL, which are of the order from less than a minute to over 11 minutes and more (e.g., Belušić et al. 2006), may be substantially shorter for mountainous winds and therefore relevant for wind engineering applications. For example, downslope windstorm gusts typically exhibit a quasi-periodic behavior, as Bora pulsations emerge in periods usually between 3 and 11 minutes (Belušić et al. 2004). It is expected that those characteristic periods may be quite different for other mountainous winds; some

examples are provided for Santa Ana (Fovell and Cao, 2017) in Fig. 10, European Alps (Cantelli et al., 2017) in Fig. 11, Ligurian downslope wind (Burlando et al. 2017) in Fig. 12, downslope wind in Japan (Kusaka and Fudeyasu 2017) in Fig. 13, Zonda (Loredo-Souza et al. 2017) in Fig 14.

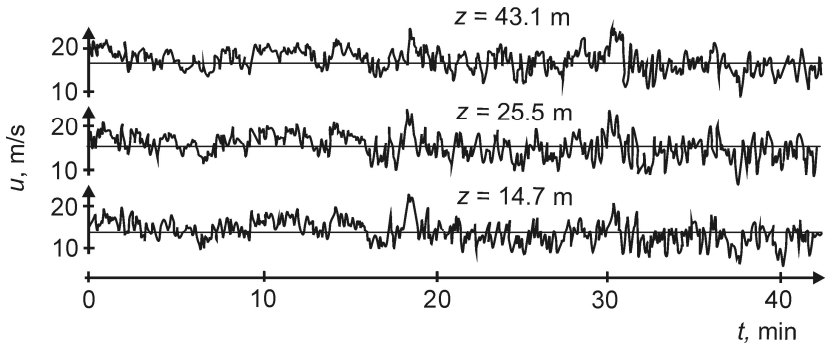

Figure 9. Quasi steady time history of the ABL wind velocity (Dyrbye and Hansen 1997, after Sigbjörnsson 1974)

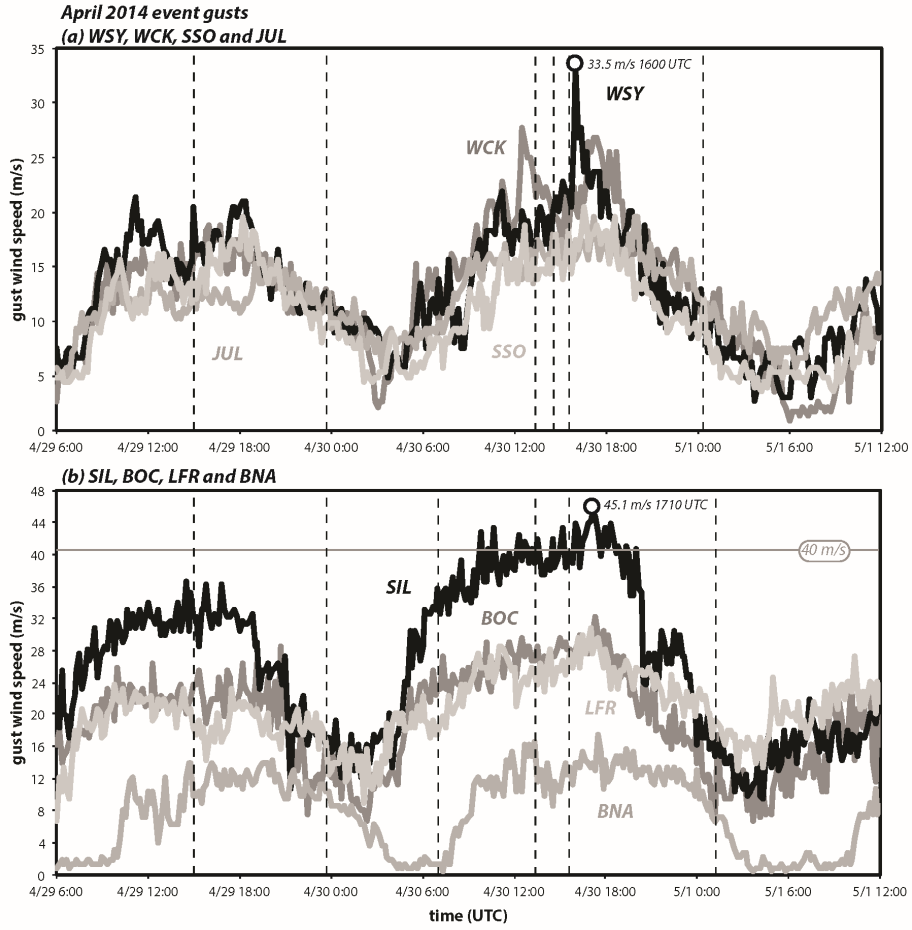

Figure 10. Velocity time history for Santa Ana (Fovell and Cao 2017)

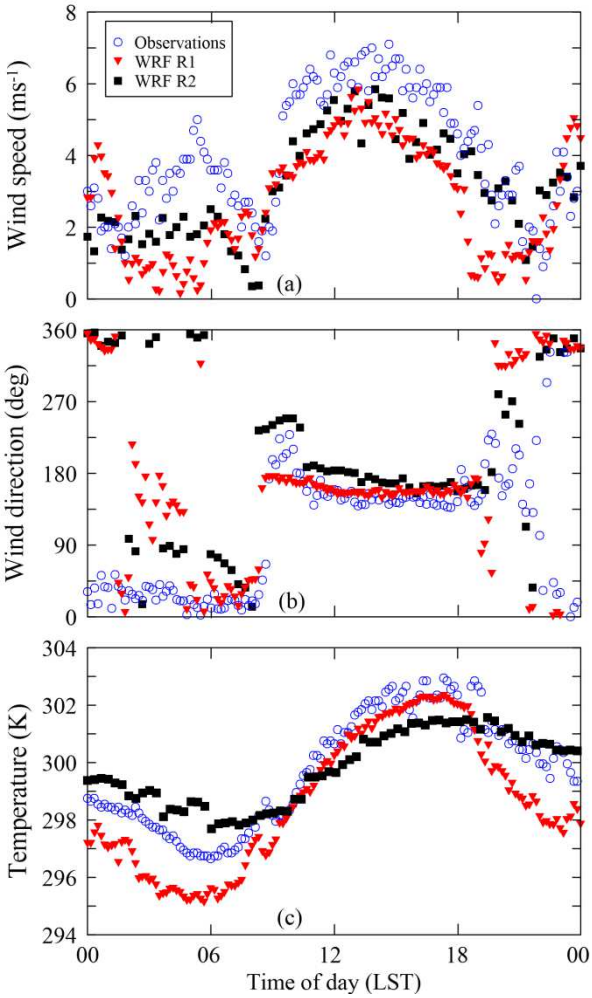

Figure 11. First panel from the top: Velocity time history for mountain winds in the Alps (Cantelli et al. 2017). Comparisons between simulated (solid symbols) and measured (open circles) (a) wind speed, (b) wind direction and (c) air temperature on 14 July 2010. All data refer to 2 m above the lake surface.

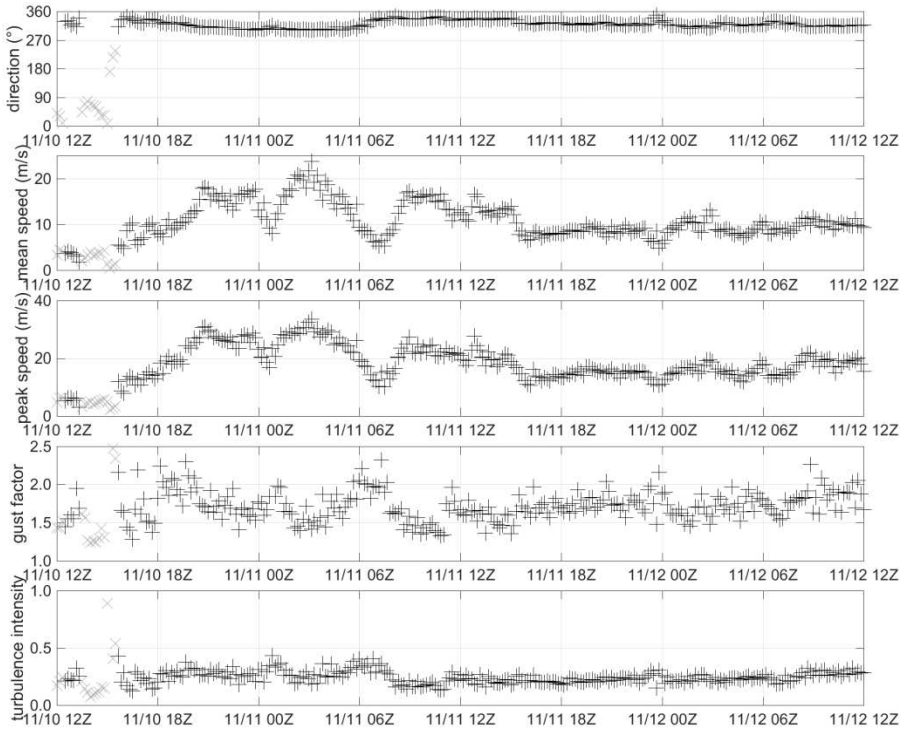

Figure 12. Second panel from the top: Velocity time history for Ligurian downslope wind (Burlando et al. 2017).

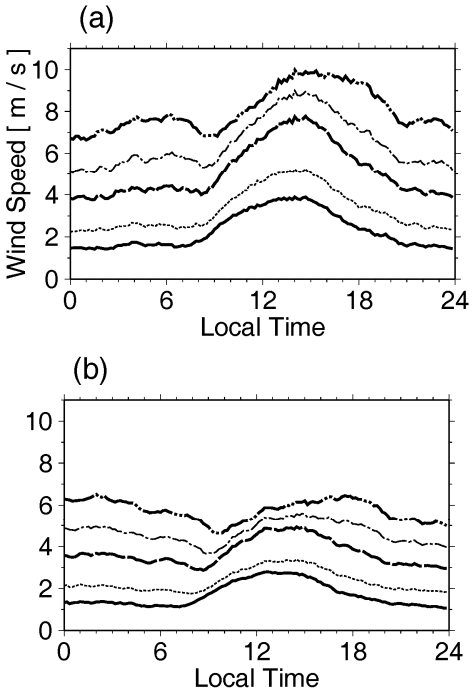

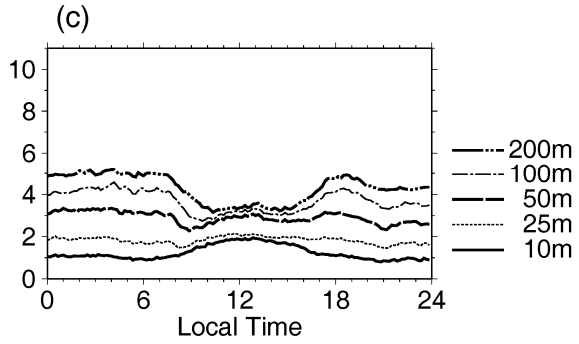

Figure 13. Velocity time history for downslope wind in Japan (Kusaka and Fudeyasu 2017).

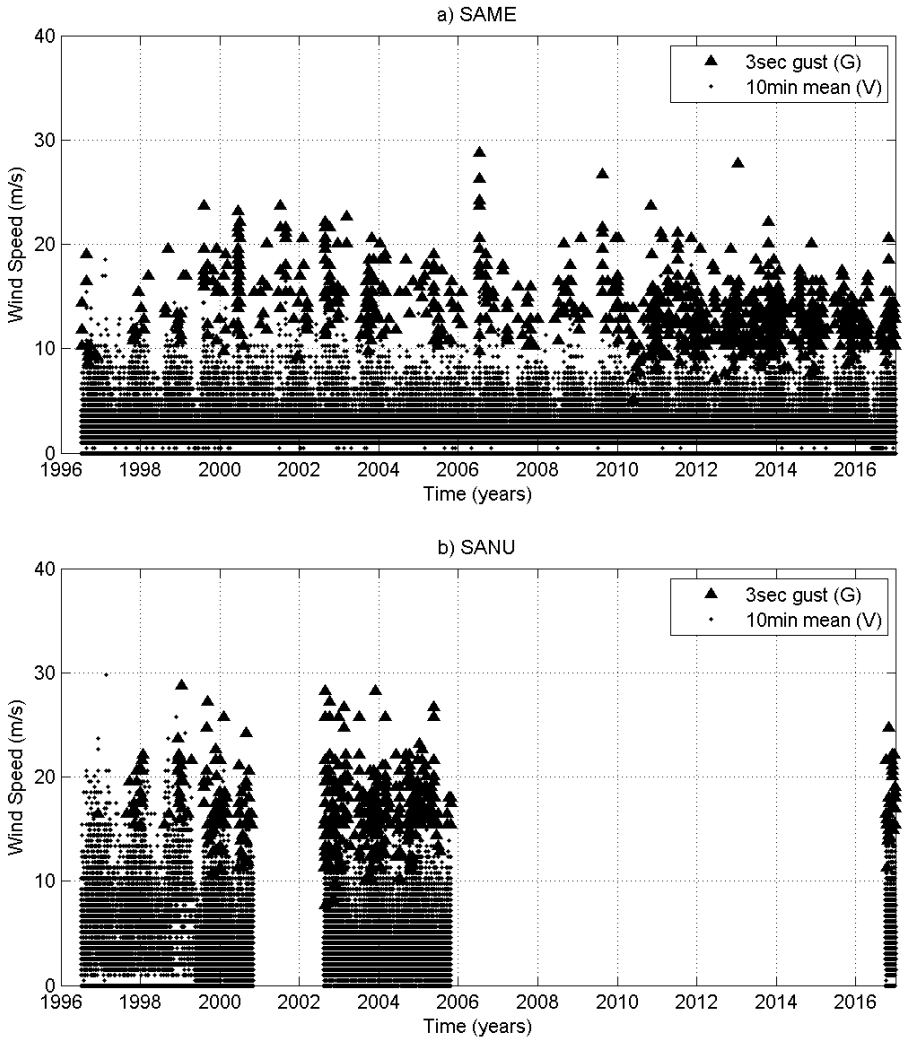

Figure 14. Velocity time history for Zonda wind in the Andes (Loredo-Souza et al. 2017).

Vertical velocity profiles

The engineers have been commonly using the logarithmic- and the power-law to represent the vertical profile of the mean wind velocity in the ABL, e.g. Simiu and Scanlan (1996), Dyrbye and Hansen (1997), Holmes (2015) and Fig. 15 adopted from Kozmar (2011a). The power-law (Hellman 1916) proved to represent well the mean velocity profile throughout the entire ABL, while the logarithmic law (Thuillier and Lappe 1964) is valid within the surface layer (lowest 10-15% of the ABL). However, this might not be the case for mountainous winds, where horizontal homogeneity assumption is typically not fulfilled and where the surface layer can be less than 1 m deep (e.g., Grisogono and Oerlemans 2001, Baklanov et al. 2011). There the mean wind may have a component from gravity as well.

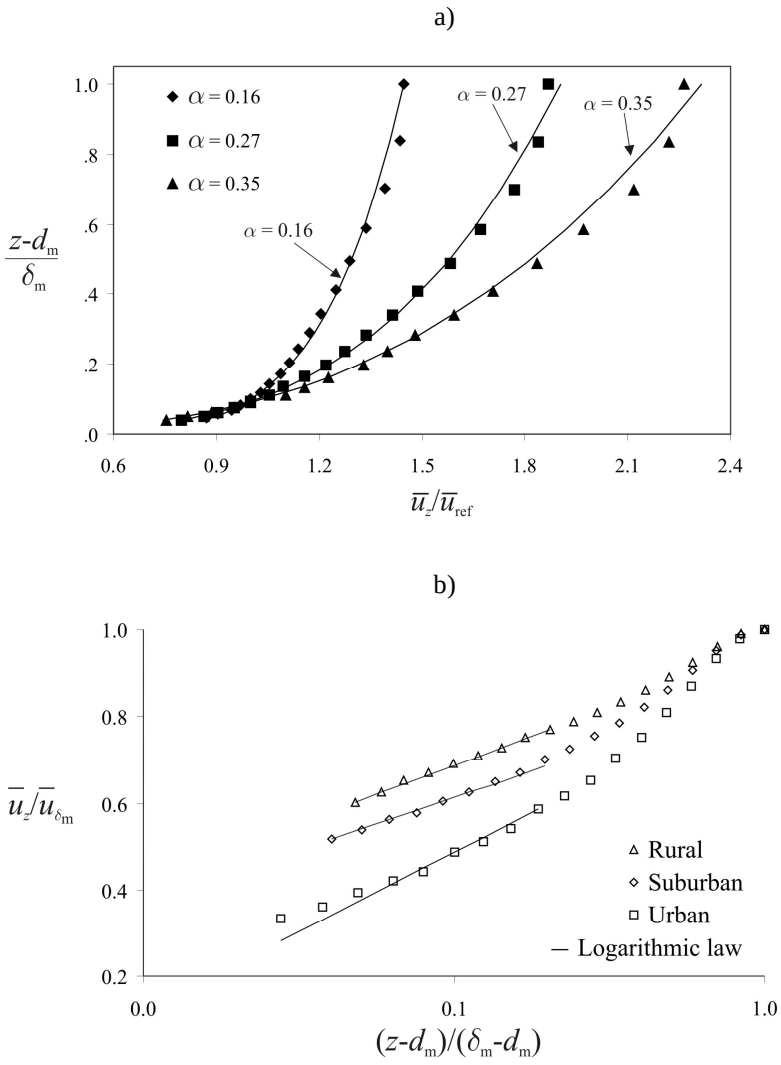

Figure 15. a) Power-law and b) logarithmic law approximations of the mean velocity profile (solid lines) after Kozmar (2011a); dots represent experimental results obtained in a boundary layer wind tunnel

While the vertical velocity profile close to the ground may agree well with the logarithmic and the power law (e.g. Lepri et al. 2017), there are substantial discrepancies from those laws further away from the ground, e.g.

Burlando et al. (2017), Kusaka and Fudeyasu (2017), Loredo-Souza et al. (2017) - all not shown, Belušić and Klaić (2004), Fovell and Cao (2017) in Figs. 16 and 17, respectively.

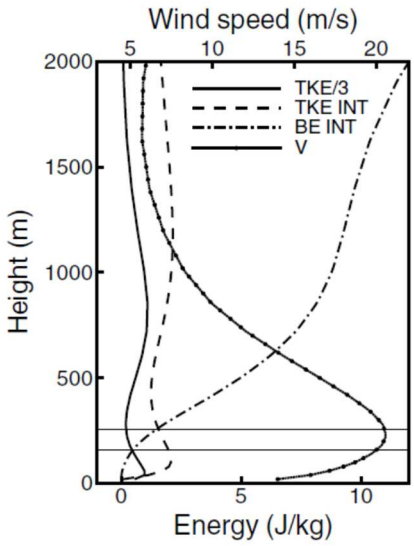

Figure 16: Vertical velocity profile of the Bora wind adapted from Belušić and Klaić (2004). Vertical profiles of 1/3 TKE (corresponding to the local vertical TKE), mean TKE in a given layer (TKE INT), buoyant energy (BE INT) and wind speed (V) at the Island of Krk, Croatia averaged over all Bora episodes during January 2002. The two horizontal lines mark the upper limits of the lower bound and gust estimate.

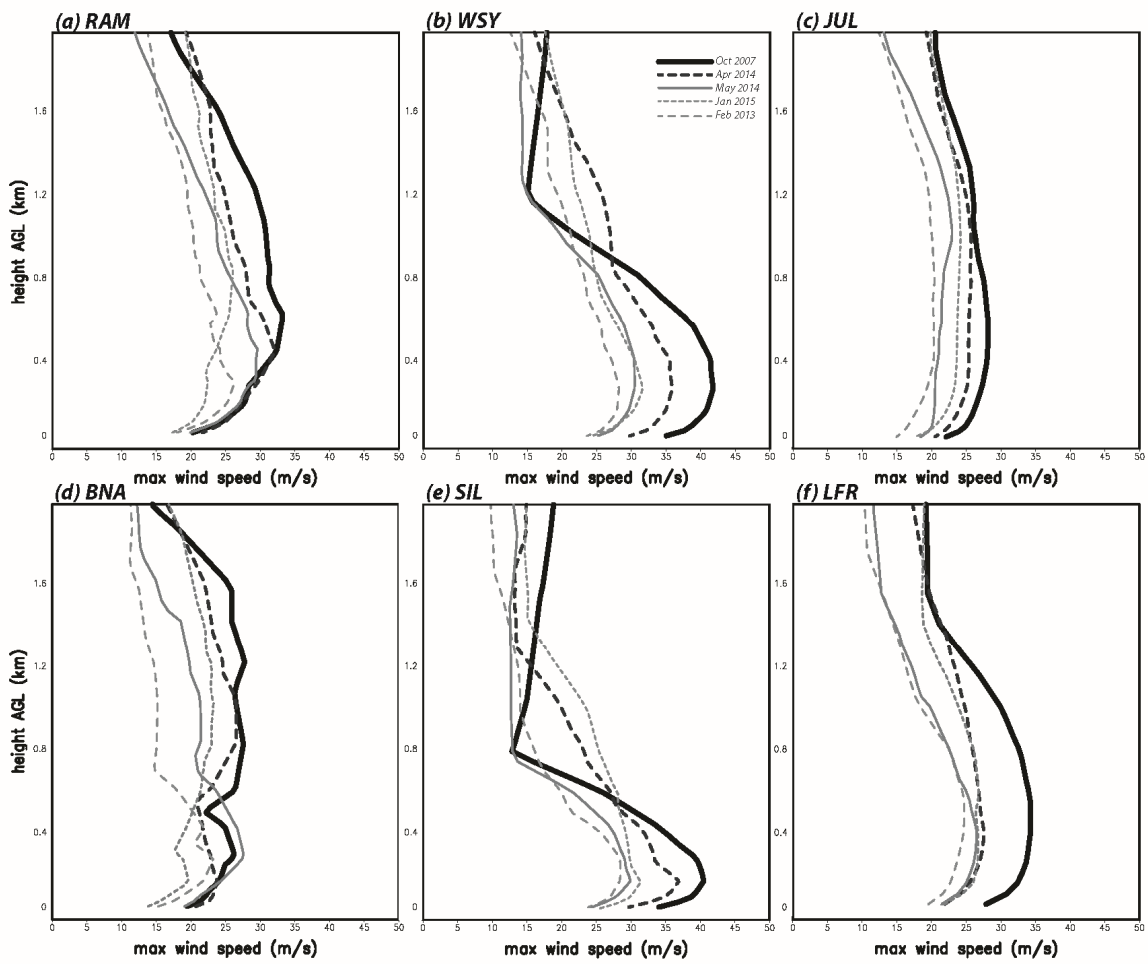

Figure 17. Vertical velocity profile of the Santa Ana wind from Fovell and Cao (2017).

Integral turbulence parameters

From the engineering perspective, integral turbulence parameters are important for dynamic performance of complex engineering infrastructure. For example, for wind loading of structures, turbulence intensity and length scales have been commonly assessed, while Reynolds shear stress is important as well when addressing air pollution transport, dispersion and dilution. It is therefore necessary to account for discrepancies between the integral turbulence parameters in the ABL and downslope windstorms. For the ABL, engineers have been commonly using recommendations from international standards and codes, e.g. ESDU, Eurocode, ASCE, where the turbulence intensity is given for various terrain types and commonly follows the trend that the longitudinal to lateral to vertical turbulence intensity is 1 : 0.75 : 0.50 (e.g. Dyrbye and Hansen 1997) or similar. The turbulence intensity has a distinct peak immediately above the ground and decreases monotonically with further increasing the height, Fig. 18, while turbulence length scales increase with increasing the height above the ground surface, Fig. 19 after. Kozmar (2011b).

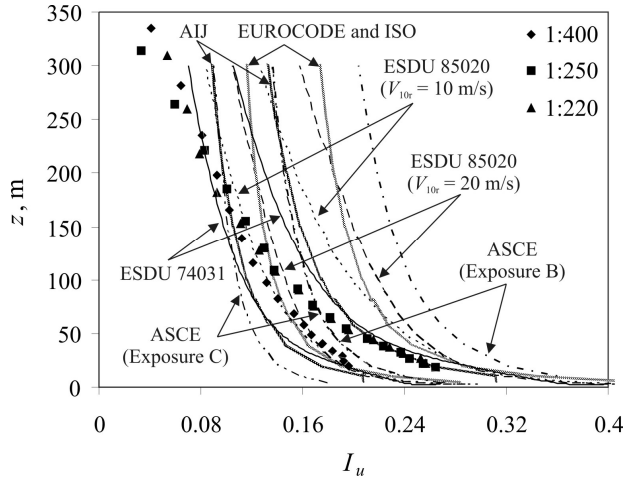

Figure 18. Profiles of the longitudinal turbulence intensity I_u in the 1:400, 1:250, and 1:220 suburban ABL wind-tunnel simulations compared to values recommended in international standards from Kozmar (2011b).

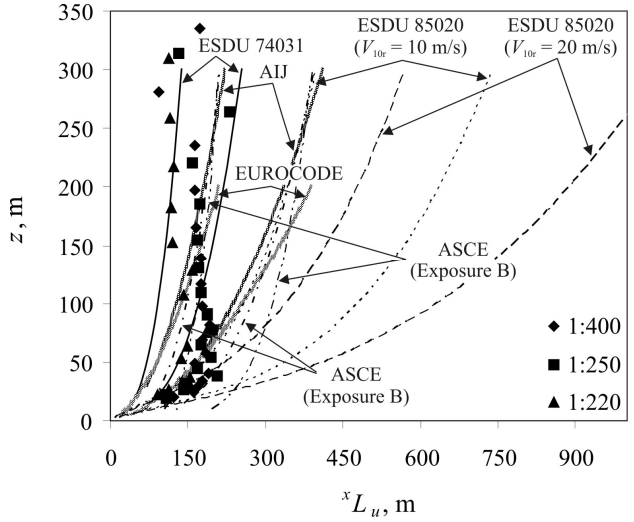

Figure 19. Profiles of the integral length scales of turbulence $^{x}L_u$ in the 1:400, 1:250, and 1:220 suburban ABL wind-tunnel simulations compared to values recommended in international standards from Kozmar (2011b).

The Reynolds shear stress remains at some constant value with increasing the height throughout the surface layer and then decreases with further increasing the height. This range of the constant shear stress (Prandtl constant-flux layer) may vary with changing the ground surface roughness, i.e. it remains constant higher up above rougher surfaces; however not higher than the surface layer top (usually 10-15% of the ABL thickness, e.g. Stull 1988, Garratt 1992). The question is how these characteristic ABL profiles behave in downslope windstorms since already weaker, e.g., katabatic winds (e.g. Grisogono and Oerlemans 2001) showed nonexistence of a typical surface layer (or it was less than 1 m deep).

In downslope windstorms, not to mention low-level jets, there are some important differences from the ABL with respect to the integral turbulence parameters that might change and broaden the concept of the engineering perspective on the ABL. While the turbulence intensity profiles appear to agree with international standards closer to the ground surface, Fig. 20, they exhibit the behavior uncommon for the ABL higher up above the

ground surface, as the turbulence intensity profiles remains fairly flat, i.e. it does not decrease with further increasing the height, Figure 21.

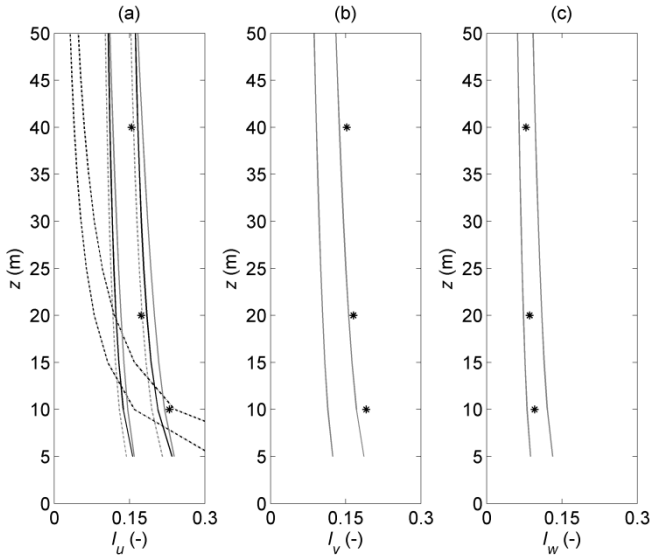

Figure 20. Vertical profile of turbulence intensity for Bora after Lepri et al. (2015). Vertical profiles of observed turbulence intensity for the averaging period of 17 min in the (a) *x*-, (b) *y*- and (c) *z*-direction calculated through the entire time record and compared with the values in international standards with the tolerance range of ±20%. Legend: star is average turbulence intensity, grey solid line is ESDU 85020 (1985) for z_0 = 0.03 m, black solid line is ISO 4354 (1997) and EN 1991 Eurocode 1 (2005), black dotted line is ASCE 7-05 (2006), grey dotted line is AIJ (2006).

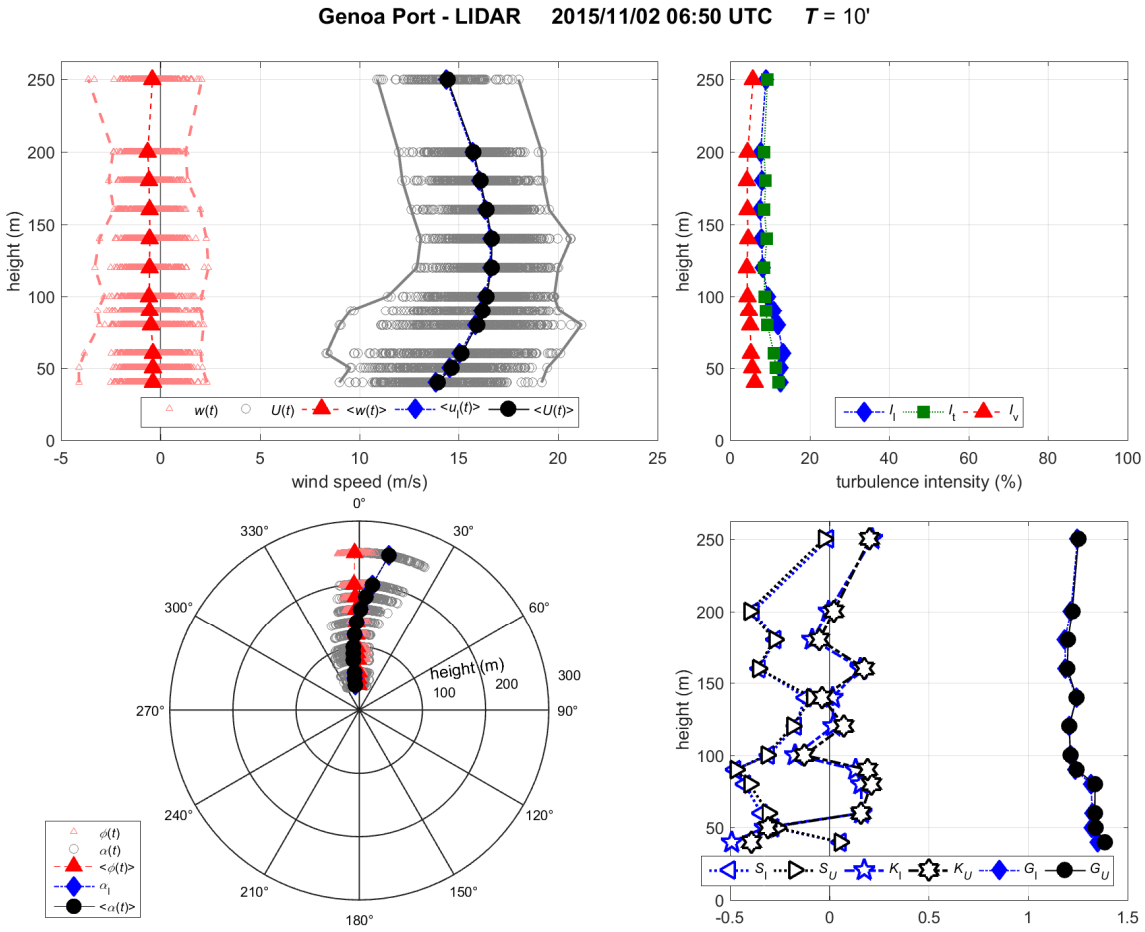

Figure 21. Top right panel: Vertical profile of turbulence intensity for Ligurian downslope wind (Burlando et al. 2017) Wind velocity field measured on November 2, 2015 at 6:50-7:00 UTC by the LiDAR in the Port of Genoa: profiles of 10-minute mean horizontal (<U>, circles), longitudinal (<u_l>, diamonds), and vertical (<w>, triangles) wind components and their variability up to 250 m above ground (top left); longitudinal, I_l, transversal, I_t, and vertical, I_v, turbulence intensities (top right); directions of the 10-minute mean horizontal (<α>, circles), longitudinal (α_l, diamonds), and vertical (ϕ, triangles) wind components and their variability as a function of height (bottom left); skewness, S, excess kurtosis, K, and gust factors, G, of the longitudinal (subscript l) and mean (subscript U) components (bottom right).

Neither the constant-flux layer is exhibited as it is the case for the ABL, e.g., Fig. 22 Lepri et al. (2015).

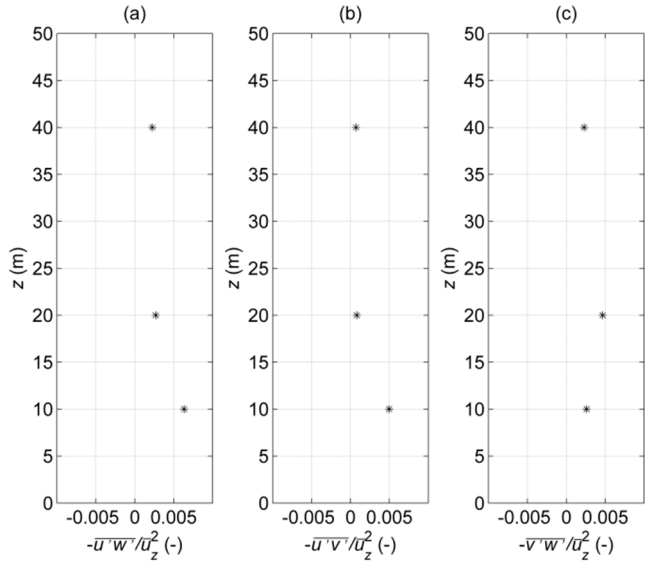

Figure 22. Vertical profile of the Reynolds shear stress for Bora after Lepri et al. (2015). Vertical profiles of the (a) $-\overline{u'w'}$, (b) $-\overline{u'v'}$, (c) $-\overline{v'w'}$ Reynolds shear stress components for the averaging period of 17 min calculated through the entire time record and normalized using the 17 min average wind velocity in the main (x) wind direction at the corresponding height for each height level.

The longitudinal turbulence length scales are generally in good agreement with the international standards ESDU 85020 (1985), EN 1991 Eurocode (2005) and ASCE 7-05(2006). The lateral and vertical turbulence length scales though are considerably larger compared to the standard ABL values, e.g. Fig. 23.

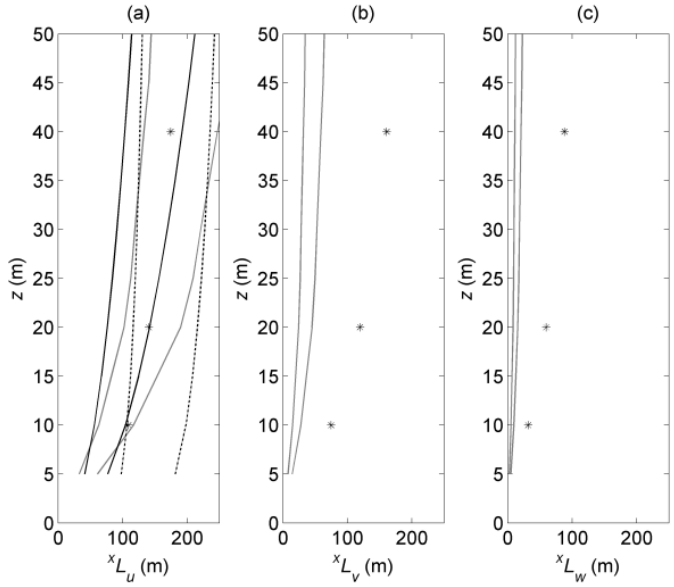

Figure 23. Vertical profiles of turbulence length scales for Bora after Lepri et al. (2015). Vertical profiles of turbulence length scales (a) ^xL_u, (b) ^xL_v and (c) ^xL_w component for the averaging time 17 min calculated through the entire time record compared with the values in international standards with tolerance range of ±30%. Legend: star is observed turbulence length scale, grey solid line is ESDU 85020 (1985) with z_0 = 0.03 m, black solid line is EN 1991 Eurocode 1 (2005), black dotted line is ASCE 7-05 (2006).

Even larger discrepancies in integral turbulence parameters in comparison with the typical ABL may be expected higher up in the atmosphere, similarly as for the mean wind velocity profiles, which are in better agreement with the ABL closer to the ground in the surface layer than higher up in the atmosphere (e.g., Smith 2002). These discrepancies may be particularly relevant for tall structures, e.g. tall buildings and wind turbines, which are designed according to the ABL characteristics because in mountainous regions those structures may experience quite different wind loads when subjected to downslope windstorms.

Wind velocity power spectra

Engineering structures have been commonly designed assuming some standard models for the velocity power spectra, e.g. von Kármán (1948), Davenport (1967), Harris (1970), e.g. Fig. 24 adopted from Kozmar (2012), which are commonly also a part of the international standards and codes. A properly selected wind velocity power spectra is very important as an input information when designing structural dynamics, as to extend the lifetime and enhance safety of those structures. Of interest is particularly the frequency range shorter than a minute.

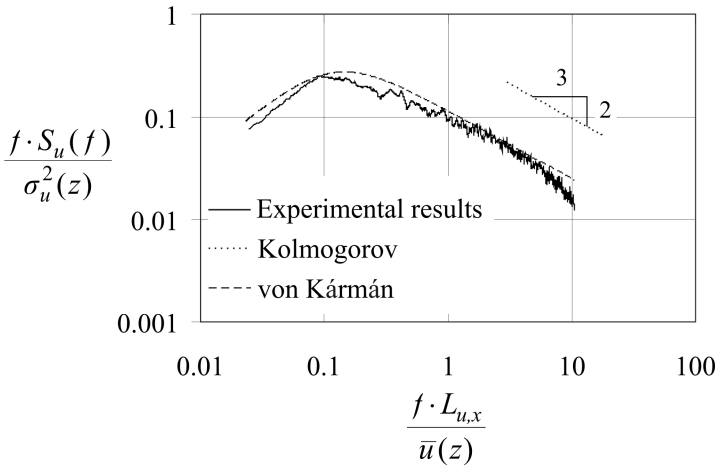

Figure 24. Power spectral density of wind velocity fluctuations in the typical ABL (Kozmar 2012).

In the areas prone to downslope windstorms, not to mention low-level jets and tropical cyclones, some other types of wind velocity spectra may be expected, e.g. Li et al. (2014). Likewise, a recent study by Babić et al. (2017) shows that the standard atmospheric spectra models can be, and often are, modified above the complex terrain by some local effects, mostly induced by the orography. This includes local mesoscale phenomena such as rotors and mountain waves. It is therefore necessary to improve the standards and codes by implementing those other types of wind spectra to be used in areas prone to downslope windstorms.

4. CONCLUDING REMARKS AND PERSPECTIVES

Characteristics of downslope windstorms in comparison with the typical atmospheric boundary layer (ABL) were critically reviewed. It was shown that the current wind engineering standards do not entirely keep up with the atmospheric physics of downslope windstorms. In particular, the atmosphere near the ground surface is

neutrally thermally stratified and the wind velocity fluctuations are much stronger in downslope windstorms than in the standard ABL. The vertical profile of wind velocity in the main wind direction close to the ground in the surface layer agrees well with the logarithmic and the power law in accordance with international standards and codes; however; there are substantial discrepancies from those laws higher up from the ground. The vertical profiles of the turbulence intensity agree with international standards closer to the ground surface, while they exhibit the behavior uncommon for the ABL higher up above the ground surface, as the turbulence intensity profiles remain fairly flat, i.e. they do not decrease with further increasing the height. Neither the constant-flux layer is as exhibited in downslope windstorms as it is the case in the ABL. While the longitudinal turbulence length scales are generally in good agreement with the international standards, the lateral and vertical turbulence length scales are considerably larger compared to the standard ABL values. There is a need for semi-empirical models of velocity power spectra in downslope windstorms comparable to the existing ABL models. It needs to be mentioned though that more work is required to further support those findings.

This new and necessary knowledge may be possibly acquired using field measurements, small-scale laboratory experiments, computational simulations and analytical modeling. Field measurements would need to be performed in locations typical for occurrence of downslope windstorms simultaneously at a large number of meteorological towers in various heights at large resolution frequency to fully account for a complex three-dimensional high-frequent flow phenomena of downslope windstorms.

Small-scale laboratory measurements have been commonly performed in boundary layer wind tunnels that are not entirely suitable to model downslope windstorms; some common issues are Reynolds number similarity, test-section blockage, large inertia of one big fan commonly used in wind tunnels of that type. Improvements in laboratory small-scale simulation of downslope windstorms can be achieved by using boundary layer wind tunnels substantially larger than those commonly used, e.g. at Politecnico di Milano (Italy) and Southwest Jiaotong University (China), transient flow field simulators, e.g. at Miyazaki University (Japan), University of Notre Dame (USA) and Florida International University (USA), three-dimensional testing chambers, e.g. at Western University (Canada), whereas characteristics of downslope windstorms may be well complemented by using the results obtained in tornado simulators, e.g. at Iowa State University (USA), Tongji University (China), University of Birmingham (UK).

While steady Reynolds-averaged Navier-Stokes (RANS) approach is not suitable for computational modeling of downslope windstorms, possibilities are available in unsteady RANS and Large Eddy Simulations (LES), whereas the Direct Numerical Simulation (DNS) would be the optimal solution; however, possibilities with this approach are still not that feasible due to a high demand for computer power that is currently not available. Meteorological state-of-the-art models almost invariably use unsteady RANS approach for operational purposes; hence, it is still inconceivable that the downslope windstorms will be predicted accurately in the near future, not to mention their climate perspectives. The latter means: the place, time of the onset, duration and cessation as well as the intensity of severe winds and the corresponding state of the ABL. In short, meteorological community is still struggling in making more regular detailed forecasts of local, intensive winds by using more advanced, e.g., LES methods.

ACKNOWLEDGMENTS

Dr. Željko Večenaj, Faculty of Science, University of Zagreb, is thanked for his constructive criticism and a comment to Figure 24. The Croatian Science Foundation HRZZ-IP-2016-06-2017 (WESLO) support is gratefully acknowledged. This work is partly financed within the Croatian-Swiss Research Program of the Croatian Science Foundation and the Swiss National Science Foundation with funds obtained from the Swiss-Croatian Cooperation program, project SWALDRIC (IZHRZ0-180587.)

REFERENCES

AIJ, 2006. AIJ Recommendations for Loads on Buildings (in English). Architectural Institute of Japan, Tokyo, Japan.

American Society of Civil Engineers (ASCE), 2006. Minimum design loads for buildings and other structures ASCE/SEI 7-05. Reston, Virginia, USA.

Babić N, Ž. Večenaj, S.F.J. de Wekker, 2017, Spectral gap characteristics in a daytime valley boundary layer. *Quart. J. Roy. Meteorol. Soc.* **143**, 2509-2523.

Baklanov, A., B. Grisogono, R. Bornstein, L. Mahrt, S. Zilitinkevich, P. Taylor, S. Larsen, M. Rotach, H.J.S. Fernando, 2011: The nature, theory and modeling of atmospheric planetary boundary layers. *Bull. Amer. Meteor. Soc.* **92**, 123-128. http://journals.ametsoc.org/toc/bams/92/2

Belušić, D., Z.B. Klaić, 2004 Estimation of bora wind gusts using a limited area model. *Tellus, Series A*: *Dynamic Meteorology and Oceanography* **56**(4), 296-307.

Belušić, D., M. Pasarić, M. Orlić, 2004: Quasi-periodic bora gusts related to the structure of the troposphere. *Quart. J. Roy. Meteorol. Soc*. **130**, 1103-1121.

Belušić, D., M. Pasarić, Z. Pasarić, M. Orlić, B. Grisogono, 2006: On local and non-local properties of turbulence in the bora flow. *Meteorol. Z.* **15**, 301-306.

Belušić, D., M Žagar, B. Grisogono, 2007: Numerical simulation of pulsations in the bora wind. *Quart. J. Roy. Meteorol. Soc*. **133**, 1371-1388, doi: 10.1002/qj.129.

Burlando M, Tizzi M, Solari G (2017) Characteristics of downslope winds in the Liguria region. *Wind and Structures* **24**(6), 613-635.

Cantelli A, Monti P, Leuzzi G, Valerio G, M. Pilotti, 2017, Numerical simulations of mountain winds in an alpine valley. *Wind and Structures* **24**(6), 565-578.

Chow, F.K., S.F.J. de Wekker and B.J. Snyder (eds), 2013: *Mountain Weather Research and Forecasting*. Springer, Dordrecht, 750 pp.

Davenport AG (1967) Gust loading factors. *Journal of Structural Division - ASCE* 93, 11-34.

Doyle, J.D. and D.R. Durran, 2004: The MAP room: Recent developments in the theory of atmospheric rotors. *Bull. Am. Meteorol. Soc*. **58**, 337-342.

Doyle, J. D. and Durran, D. R. 2007: Rotor and subrotor dynamics in the lee of three dimensional terrain. *J. Atmos. Sci*. **64**, 4202-4221.

Doyle, J., V. Grubišić, W.O.J. Brown, S.F.J. de Wekker, A. Dörnbrack, Q. Jiang, S.D. Mayor and M. Weissmann, 2009: Observations and numerical simulations of subrotor vortices during T-REX. *J. Atmos. Sci*. **66**, 1229-1249.

Durran, D.R., 1986; Another look at downslope windstorms. Part I: the development of analogs to supercritical flow in an infinitely deep, continuously stratified fluid. *J. Atmos. Sci.* **43**, 2527-2543.

Durran, D.R., 1990: Mountain waves and downslope winds. *Atmospheric Processes Over Complex Terrain*. Edited by W. Blumen. Am. Meteorol. Soc. 59-81. (323 pp.)

Dörnbrack, A, 1998: Turbulent mixing by breaking gravity waves. *J. Fluid Mech.* **375**, 113-141.

Dyrbye, C., Hansen, S., 1997. Wind loads on structures, Wiley, New York, USA.

Enger, L. and B. Grisogono, 1998: The response of bora-type flow to sea surface temperature. *Quart. J. Roy. Meteorol. Soc*. **124**, 1227-1244.

ESDU Data Item No. 85020, 1985. Characteristics of atmospheric turbulence near the ground. Part Ii: single point data for strong winds (neutral atmosphere). Engineering Science Data Unit, London, UK.

EN 1991 Eurocode 1, 2005. Actions on structures – General actions – Part 1 – 4: Wind actions.

Fovell, R.G., Cao Y (2017) The Santa Ana winds of Southern California: Winds, gusts, and the 2007 Witch fire. Wind and Structures 24(6), 529-564.

Garratt JR (1992) The Atmospheric Boundary Layer. Cambridge University Press, Cambridge, UK.

Grisogono, B. and J. Oerlemans, 2001: A theory for the estimation of surface fluxes in simple katabatic flows. *Quart. J. Roy. Meteorol. Soc.* **127**, 2725-2739.

Grisogono, B. and D. Belušić, 2009: A review of recent advances in understanding the meso- and micro-scale properties of the severe Bora wind. *Tellus*, **61A**, 1-16.

Grubišić, V. and M. Orlić, 2007: Early observations of rotor clouds by Andrija Mohorovičić. *Bull. Amer. Meteorol. Soc*. **88**, 693-700.

Grubišić, V. and B.J. Billings, 2008: Summary of the Sierra Rotors Project wave and rotor events. *Atmos. Sci. Let*. **9**(4), 176–181. doi:10.1002/asl.200

Grubišić, V., J.D. Doyle, J. Kuettner, S. Moggs, R.B. Smith, C.D. Whiteman, R. Dirks, S. Czyzyk, S.A. Cohn, S. Vosper, M. Weissmann, S. Haimov, S.F.J. de Wekker, L.L. Pan and F.K. Chow, 2008: The terrain-induced rotor experiment. *Bull. Amer. Meteor. Soc.* **89**, 1513-1533.

Harris RI (1970) The nature of the wind, Seminar on Modern Design of Wind-Sensitive Structures. Construction Industry Research & Information, CIRIA, London, 29-35.

Hellman, G. (1916), Über die Bewegung der Luft in den untersten Schichten der Atmosphäre, *Meteorol. Z.*, 34, 273-285.

Holmes JD (2015) Wind Loading of Structures, CRC Press, Boca Raton, FL, USA..

Hunt, J.C.R., Y, Feng, P.F. Linden, M.D. Greenslade and S.D. Mobbs, 1997: Low-Froude-number stable flows past mountains. *Il Nuovo Cimento*, **20**, 261-272.

Hunt, J.C.R., H. Olafsson and P. Bougeault, 2001: Coriolis effects on orographic and mesoscale flows. . *Quart. J. Roy. Meteorol. Soc.* **127**, 601-633.

ISO 4354, 1997. Wind actions on structures. International standard organization.

Jackson, P.L., G. Mayr and S. Vosper, 2013: Dynamically driven winds. *Mountain Weather Research and Forecasting*. Edited by Chow, F.K., S.F.J. de Wekker and B.J. Snyder. Springer, Dordrecht, 121-218 (750 pp.).

Jurčec, V., 1981. On mesoscale characteristics of bora conditions in Yugoslavia. Pure and applied Geophysics 119(3), 640–657.

Klemp, J.B. and D.R. Durran, 1987: Numerical modelling of Bora winds. *Meteorol. Atmos. Phys.* **36**, 215-227.

Klemp, J.B. and D.K. Lilly, 1978: Numerical simulation of hydrostatic mountain waves. *J. Atmos. Sci*. **35**, 78-107.

Kozmar H (2011a) Characteristics of natural wind simulations in the TUM boundary layer wind tunnel. *Theor Appl Climatol* 106, 95-104.

Kozmar H (2011b) Wind-tunnel simulations of the suburban ABL and comparison with international standards. *Wind and Structures* 14(1), 15-34.

Kozmar H (2012) Physical modeling of complex airflows developing above rural terrains. *Environ Fluid Mech* 12, 209-225.

Kusaka H, Fudeyasu H (2017) Review of downslope windstorms in Japan. *Wind and Structures* 24(6), 637-656.

Lepri P, Kozmar H, Večenaj Ž, Grisogono B (2014) A summertime near-ground velocity profile of the Bora wind, *Wind and Structures* 19(5), 505-522.

Lepri P, Večenaj Ž, Kozmar H, Grisogono B (2015) Near-ground turbulence of the Bora wind in summertime, *Journal of Wind Engineering and Industrial Aerodynamics* 147, 345-357.

Lepri P, Večenaj Z, Kozmar H, Grisogono B (2017) Bora wind characteristics for engineering applications, *Wind and Structures* 24(6), 579-611.

Li L, Kareem A, Hunt J, Xiao Y, Zhou C, Song L (2014) Turbulence Spectra for Boundary-Layer Winds in Tropical Cyclones: A Conceptual Framework and Field Measurements at Coastlines. *Boundary-Layer Meteorology* 154(2), 243-263.

Lilly, D.K., 1978: A severe downslope windstorm and aircraft turbulence event induced by a mountain wave. *J. Atmos. Sci*. **35**, 59-77.

Lilly, D.K. and J.B. Klemp, 1979: The effects of terrain shape on nonlinear hydrostatic mountain waves. *J. Fluid. Mech*. **95**, 241-261.

Loredo-Souza AM, Wittwer AR, Castro HG, Vallis MB (2017) Characteristics of Zonda wind in South American Andes. *Wind and Structures* 24(6), 657-677.

Mayr, G.J., D. Plavcan, L. Armi, A. Elvidge, B. Grisogono, K. Horvath, P. Jackson, A. Neururer, P. Seibert, J.W. Steenburgh, I. Stiperski, A. Sturman, Ž. Večenaj, J. Vergeiner, S. Vosper and G. Zängl, 2018: The community Foehn classification experiment. *Bull. Amer. Meteor. Soc.* doi:10.1175/BAMS-D-17-0200.1, in press. https://journals.ametsoc.org/doi/pdf/10.1175/BAMS-D-17-0200.1

Mohorovičić, A. 1889: Interessante Wolkenbildung űber der Bucht von Buccari (with a comment from the editor J. Hann). *Meteorol. Z.* **24**, 56-58.

Ólafsson, H. and P. Bougeault, 1996: Nonlinear flow past an elliptic mountain ridge. *J. Atmos. Sci*. **53**, 2465-2489.

Pope, S.B., 2000: *Turbulent Flows*. Cambridge Univ. Press. 749 pp.

Poulos, G.S., J.E. Bossert, T.B. McKee and R.A. Pielke, 2000: The interaction of katabatic flow and mountain waves. Part I: Observations and idealized simulations. *J. Atmos. Sci*. **57**, 1919-1936.

Poulos, G.S., J.E. Bossert, T.B. McKee and R.A. Pielke, 2007: The interaction of katabatic flow and mountain waves. Part II: Case study analysis and conceptual model. *J. Atmos. Sci*. **64**, 1857-1879.

Richner, H. and P. Hächler, 2013: Understanding and forecasting Alpine Foehn. *Mountain Weather Research and Forecasting*. Edited by Chow, F.K., S.F.J. de Wekker and B.J. Snyder. Springer, Dordrecht, 219-260 (750 pp.).

Rogers, D.P., E.C. Dorman, K.A. Edvards, I.M. Brooks, W.K. Melville, S.D. Burk, W.T. Thompson, T. Holt, L.M. Strom, M. Tjernstrom, B. Grisogono, J.M. Bane, W.A.Nuss, B.M. Morley and A.J. Schanot, 1998: Highlights of coastal waves 1996. *Bul. Am. Meteorol. Soc*. **79**, 1307-1326.

Rotach, M. and D. Zardi, 2007: On the boundary-layer structure over highly complex terrain: Key findings from MAP. *Quart. J. Roy. Meteorol. Soc*. **133**, 937-948.

Sachsperger, J., S. Serafin and V. Grubišić, 2015: Lee waves on the boundary-layer inversion and their dependence on free-atmospheric stability. *Frontiers Earth Sci*. **3**, 14-24, doi: 10.3389/feart.2015.00070

Scinocca, J.F. and W.R. Peltier, 1993: The instability of Long's stationary solution and the evolution toward severe downslope windstorm flow. Part I: nested grid numerical simulations. *J. Atmos. Sci*. **50**, 2245-2263.

Scinocca, J.F. and W.R. Peltier, 1994: The instability of Long's stationary solution and the evolution toward severe downslope windstorm flow. Part II: the application of finite-amplitude local wave-activity flow diagnostics. *J. Atmos. Sci*. **51**, 623-653.

Serafin S, Adler B, Cuxart J, De Wekker SFJ, Gohm A, Grisogono B, Kalthoff N, Kirshbaum DJ, Rotach MW, Schmidli J, Stiperski I, Večenaj Ž and Dino Zardi (2018) Exchange Processes in the Atmospheric Boundary Layer Over Mountainous Terrain. *Atmosphere* **9**(3), 102.

Sigbjörnsson, R., 1974: On the theory of structural vibrations due to natural wind. Department of Structural Engineering, Technical University of Denmark, Report R 59.

Simiu E, Scanlan RH (1996) Wind Effects on Structures: Fundamentals and Applications to Design. John Wiley & Sons, New York, USA.

Smith, R.B., 1977: The steepening of hydrostatic mountain waves. *J. Atmos. Sci*. **34,** 1634-1654.

Smith, R.B., 1978: A measurement of mountain drag. *J. Atmos. Sci*. **35**, 1644-1654.

Smith, R.B., 1979: The influence of mountains on the atmosphere. *Adv. Geophys.* **21**, 87-230. DOI is 10.1016/S0065-2687(08)60262-9

Smith, R.B., 1985: On severe downslope winds. *J. Atmos. Sci*. **42**, 2597-2603.

Smith, R.B., 1987: Aerial observations of the Yugoslavian Bora. *J. Atmos. Sci*. **44**, 269-297.

Smith, R.B., 2002: Stratified flow over topography. *Environmental Stratified Flows*. (Ed. R. Grimshaw) Kluwer, 284 pp (119-159).

Strauss, L., S. Serafin and V. Grubišić, 2016: Atmospheric rotors and severe turbulence in a long deep valley. *J. Atmos. Sci.* **73**, 1481-1506.

Stull, R.B., 1988: *An Introduction to Boundary Layer Meteorology*. Kluwer Academic Publishers, Dordrecht, the Netherlands, 666 pp.

Sun, J., C. J. Nappo, L. Mahrt, D. Belušić, B. Grisogono, D. R. Stauffer, M. Pulido, C. Staquet, Q. Jiang, A. Pouquet, C. Yague, B. Galperin, R. B. Smith, J. J. Finnigan, S. D. Mayor, G. Svensson, A. A. Grachev and W. D. Neff, 2015: Review of wave-turbulence interactions in the stable atmospheric boundary layer. *Rev. Geophys.* **53,** 956-993. http://onlinelibrary.wiley.com/doi/10.1002/2015RG000487/pdf

Šoljan, V., A. Belušić, K. Šarović, I. Nimac, S. Brzaj, J. Suhin, M. Belavić, Ž. Večenaj and B. Grisogono, 2018: Micro-scale properties of different bora types. *Atmosphere*, 9 (4), 116-141. http://www.mdpi.com/2073-4433/9/4/116

Teixeira, M.A.C., P.M.A. Miranda and R.M.Cardoso, 2008: Asymptotic gravity wave drag expressions for non-hydrostatic rotating flow over a ridge. *Quart. J. Roy. Meteorol. Soc.* **134**, 271-276.

Teixeira, M.A.C., 2014: The physics of orographic gravity wave drag. *Front. Phys.* **2**, 1-24.

Teixeira, M.A.C., D.J. Kirshbaum, H. Ólafsson, P.F. Sheridan, I. Stiperski (eds), 2016: The atmosphere over mountainous regions. Lausanne: Frontiers Media. doi: 10.3389/978-2-88945-016-9

Thuillier, R.H. and U.O. Lappe, 1964: Wind and temperature profile characteristics from observations on a 1400 ft tower. *J. Appl. Meteor*.**3**, 299–306.

Von Kármán T (1948) Progress in the statistical theory of turbulence. *Journal of Maritime Research* 7.

WAS (2017) Wind and Structures **24**(**6**) Special issue on Characteristics of Downslope Windstorms for Engineering Applications.

Wyngaard, J.C., 2010: *Turbulence in the Atmosphere*. Cambridge Univ. Press. Princeton, 393.

Zardi, D. and C.D. Whiteman, 2013: Diurnal mountain wind systems. *Mountain Weather Research and Forecasting*. Edited by Chow, F.K., S.F.J. de Wekker and B.J. Snyder. Springer, Dordrecht, 35-119 (750 pp.).

Zhong, S. and C.D. Whiteman, 2008: Downslope flows on a low-angle slope and their interactions with valley inversions. Part II: Numerical modeling. *J. Appl. Meteor. Climatol*. **47**, 2039-2057.

Yoshino, M.M., 1976: *Local Wind Bora*. Univ. of Tokyo press. 289 pp.